THE JOURNAL OF PHYSICAL CHEMISTRY C LETTERS

2008, *112,* 13328–13331
Published on Web 08/07/2008

Nanostructure-Dependent Metal−Insulator Transitions in Vanadium-Oxide Nanowires

Jeong Min Baik,† Myung Hwa Kim,† Christopher Larson, Alec M. Wodtke,* and Martin Moskovits*

Department of Chemistry & Biochemistry, University of California, Santa Barbara, California 93106

Received: June 23, 2008; Revised Manuscript Received: July 19, 2008

Single-crystal VO_2 nanowires were synthesized using atmospheric-pressure and physical vapor deposition and outfitted with electrodes for current−voltage measurements. The Mott insulator-to-metal transition temperatures of several nanowires with varying lateral dimensions were determined by measuring the voltage values at which the sharp current step, signaling that the occurrence of the insulator-to-metal or the reverse transitions, had taken place. The observed Mott transition temperatures, which ranged between 62 and 70 °C for the nanowires measured, trended downward with decreasing nanowire width. We ascribe this to strong interactions between the nanowire and the underlying silica substrate. However, the scatter in the Mott-temperature versus nanowire width exceeded the experimental uncertainty in the values of the Mott temperature, indicating that other parameters also contribute to the precise value of the Mott transition temperature of nanostructured VO_2.

Introduction

Vanadium dioxide (VO_2) is the iconic material which undergoes a Mott metal−insulator transition at a temperature of 68 °C in the bulk.[1,2] As a result, vanadium oxide has been proposed as a suitable material for constructing thermochromic devices and Mott field-effect transistors.[3−6] In general, the Mott transition in VO_2 occurs alongside a structural phase transition from monoclinic (the insulator or semiconductor phase) at temperatures below the Mott transition temperature to tetragonal (the metallic phase) above that temperature, which is accompanied by several orders of magnitude jump in conductivity.

The connection between the structural phase transition and the Mott transition has been considered in a number of publications.[6−8] Because the Mott transition in these systems is brought on by a change in crystalline structure wherein the two phases differ in density, the application of hydrostatic pressure, or, more generally, of stress by whatever means, is expected to have a significant effect on the Mott transition temperature, the sharpness of the transition, and other physical and structural consequences. The Mott transition can also be observed as a result of resistive heating of a VO_2 film or wire by applying an appropriate DC bias across the device while keeping the system at an ambient temperature below the structural transition temperature.[9,10] Because in most structures the local resistance can vary from location to location, Mott transitions induced by the application of a DC bias might bring about local changes in structure accompanying the Mott transition rather than global structural changes that are induced by changes in ambient temperature and pressure.

In this paper, we report the synthesis by atmospheric pressure, physical vapor deposition (APPVD) of single-crystal VO_2 nanowires with a narrow width distribution. The nanowires were configured as single-nanowire resistors, and their current−voltage characteristics were measured as a function of ambient temperature. The current passing through the nanowire, which is held at a temperature below the Mott transition, resistively heats the nanowire, causing the current passing through the nanowire to increase abruptly at the voltage value at which the nanowire's temperature first reaches the Mott transition. This transition occurs at an applied voltage which depends on the ambient temperature. This fact, which can be used to improve the precision with which the Mott transition temperature is determined, was used to probe the Mott transition temperature for nanowires with various dimensions.

Experimental Section

Vanadium oxide nanowires were grown by APPVD on single crystal (100) Si wafers covered with a 200nm thick, thermally grown SiO_2 layer. The wafers were first cleaned in the standard manner.[11] A total of 0.1 g of fine meshed VO_2 (99.9%, Aldrich) powder was placed at the center of a 10 cm long quartz boat without further purification. The SiO_2/Si substrate was then located in the quartz boat approximately 5 mm from the VO_2. The quartz boat was then located at the center of quartz tube furnace and high purity He carrier gas (99.999%) was a flowed through the furnace as 300 sccm. The furnace temperature was increased to a temperature in the range of 550−650 °C. After 10∼60 min of growth the samples were allowed to cool to room temperature in He and the nanowire-covered substrate removed from the furnace. High yields of good-quality VO_2 nanowires were only obtained when the procedure was conducted at atmospheric pressure.

Field-emission scanning electron microscopy (FEI Sirion XL30-FEG) was used to observe the morphologies of the VO_2 nanowires. The structural properties were determined by the energy dispersive X-ray spectroscopy, X-ray diffraction, and single nanowire Raman spectroscopy.

* To whom correspondences should be addressed. E-mail: mmoskovits@itsc.ucsb.edu; wodtke@chem.ucsb.edu.
† These authors contributed equally to this work.

10.1021/jp805537r CCC: $40.75

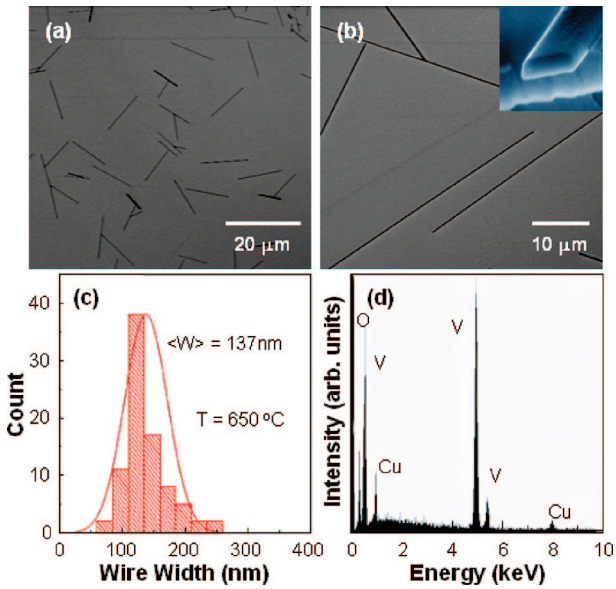

Figure 1. (a) Low- and (b) high-magnification SEM images of VO_2 nanowires synthesized on a SiO_2 substrate at 650 °C using atmospheric-pressure, physical vapor deposition. (Inset of b) SEM image showing the near-rectangular cross section of a VO_2 nanowire. The size asymmetry in the upper and lower edge of the nanowire was observed for all nanowires imaged, implying that nanowire-substrate interactions (probably operating during synthesis) affect the structure of the nanowire. (c) Histogram depicting the nanowire width distribution based on measurements on high-magnification SEM images of many nanowires. The mean wire width was found to be 137 (±34) nm. (d) Energy dispersive X-ray spectrum from an individual VO_2 nanowire, showing only vanadium and oxygen peaks. (The Cu comes from the TEM grid used as support.) The V/O atomic ratio remained unchanged as the SEM gun moves along the nanowire.

Results and Discussion

Scanning electron microscopy (SEM) imaging (Figure 1, panels a and b) shows the product (of a reaction carried out at 650 °C) to consist of long, randomly oriented VO_2 nanowires. The lengths of most of the nanowires fall in the range 20−150 μm. The mean nanowire width, measured at the nanowire−SiO_2 interface for a representative number of nanowires, was determined by SEM (Figure 1a) to be 137 (±34) nm. SEM images of nanowire cross-sections (e.g., inset to Figure 1b) shows the nanowire's lateral dimension (width) as measured at the substrate-nanowire interface to be larger than at the upper (i.e., nanowire-air) interface, implying that interfacial VO_2−SiO_2 interactions are among the structure-determining contributors affecting the nanowire growth process. Energy dispersive X-ray (EDX) fluorescence spectra from individual VO_2 nanowires showed the presence of vanadium and oxygen exclusively (Figure 1d).

Raman spectra of single nanowires on sapphire (1102) excited by 633 nm laser light, clearly show the nanowires to be single-crystal monoclinic VO_2. The Raman spectra (Figure 2a) are dominated by two sharp peaks at 191 and 223 cm^{-1} and a broad peak at 615 cm^{-1}, the latter corresponding to an A_{1g} V−O stretching mode.[12] All the Raman bands seen in the spectrum can be attributed to monoclinic VO_2 and accord with previously reported spectra of VO_2.[13,14] The nanowires were also examined using X-ray diffraction (XRD) (Figure 2b) further corroborating the aforementioned structure.[15] The most striking feature is that only diffraction peaks corresponding to (011) and (022) planes are observed, indicating that the VO_2 nanowires grow along a preferential direction.

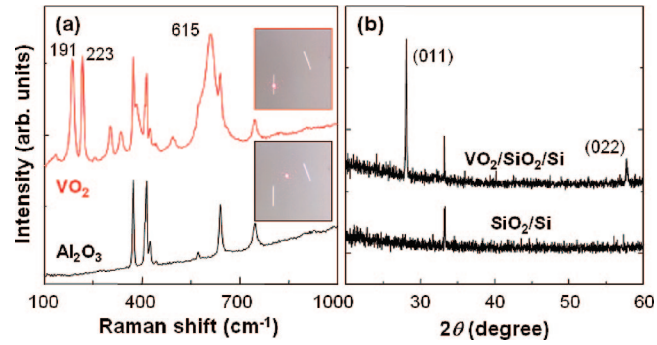

Figure 2. (a) Raman spectra of a single nanowire on a sapphire substrate. (Inset) White light optical images of the nanowires recorded prior to the Raman measurement. The location of the laser spot is shown. The Raman spectrum is unchanged as different regions along the nanowire are probed indicating the nanowire's uniformity. (b) X-ray diffraction patterns of as-grown VO_2 nanowires supported on a SiO_2/Si substrate (upper curve) and of the substrate alone (lower curve). Only (011) and (022) reflections are observed, indicating that the VO_2 nanowires have a preferential growth direction. These XRD peaks correspond to monoclinic VO_2 nanowires with lattice constants a = 5.75 Å, b = 4.52 Å, c = 5.38 Å, and β = 122.6° (JCPDS file 44−0252). The peak at 33.2° is due to the substrate.

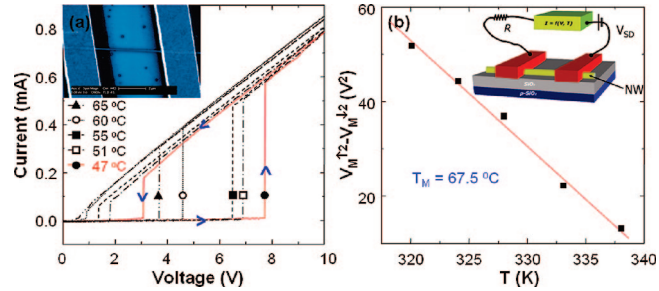

Figure 3. (a) $I-V$ curves measured at ambient temperature in the range of 47 − 65 °C by varying the applied bias both from low to high voltage values and in the reverse direction. (Inset) SEM image of VO_2 nanowire configured with electrodes on the SiO_2/Si substrate on which it was synthesized. The height and width of the nanowire shown is 140 and 70 nm, respectively. (b) A plot of the difference in the square of the voltages at which the Mott transition occurs in the upward and downward directions vs ambient temperature (ΔV_M^2 vs T_0). (Inset) Cartoon of the device used to carry out these measurements.

Electrical contacts were deposited onto individual VO_2 nanowires residing on the SiO_2/Si substrate on which they were grown. The Ti/Au (10/500 nm) electrodes were patterned by photolithography and deposited using conventional e-beam metal vapor deposition. $I-V$ measurements were carried out in a two-terminal configuration in series with a 10 kΩ resistor (inset of figure 3b). Figure 3a shows a number of $I-V$ curves carried out at various values of the ambient temperature in the range 47−65 °C. At low values of the applied voltage, the current increased linearly with increasing voltage with a slope corresponding to a conductance value of 1.05×10^{-6} Ω^{-1} characteristic of VO_2 in its insulator phase. During this initial phase of the $I-V$ measurements resistive heating ($\sim V^2/R$) is provided by the rather high resistance of the nanowire. Eventually a voltage, $V_M^{\uparrow}$, is reached at which the current rises precipitately. Presumably at this voltage the resistive heating is sufficient to cause the temperature to reach the Mott transition temperature over a significant portion of the nanowire. (The superscripting convention on $V_M^{\uparrow}$, is chosen such that the up-pointing arrow refers to an experiment in which the bias across the nanowire is increased from low to high values.) Increasing the bias voltage beyond $V_M^{\uparrow}$ causes the current to increase linearly but with a

slope characteristic of the higher conductance of the nanowire in its metallic phase (0.95×10^{-3} Ω^{-1}). On reversing the direction of the voltage scan the current decreases. It continues to decrease on the higher-conductance curve past $V_M^{\uparrow}$ until the voltage reaches the value $V_M^{\downarrow}$. Because in its metallic state the nanowire resistance is smaller, the power dissipated in the nanowire at a given voltage is greater than it would have been for a nanowire in its insulator phase. Accordingly, one needs to reduce the voltage to this lower value for the resistive heating to decrease sufficiently for the temperature of the nanowire to drop to the Mott transition temperature. Not unexpectedly, the voltage difference, $V_M^{\uparrow} - V_M^{\downarrow}$ decreases as the ambient temperature is increased toward the Mott transition temperature. This fact was used to determine the Mott transition temperature with good precision in several nanowires of varying widths.

Assuming the power dissipated in the VO_2 nanowire is due entirely to resistive heating counterbalanced by conductive losses, the power balance equation is given by

$$\frac{dQ}{dt} = \frac{V_c^2}{R_c} - k(T - T_0) \tag{1}$$

where k is a collection of parameters and includes the influence of the thermal conduction coefficient, the mass and heat capacity of the nanowire and geometrical constants, T and T_0, are respectively the temperature of the nanowire and the ambient temperature, and V_c and R_c are respectively the voltage drop across the nanowire and its resistance. At steady state $dQ/dt = 0$ and eq 1 can be rearranged to

$$T = T_0 + \frac{V_c^2}{kR_c} \tag{2}$$

Assuming that the nanowire is connected with leads to a voltage source and that there is a junction resistance R_0, the voltage drop across the nanowire is related to the voltage imposed on the leads, V, through the relationship

$$V_c = \frac{VR_c}{R_0 + R_c} \tag{3}$$

Substituting eq 3 into eq 2 produces

$$T = T_0 + \frac{R_c}{k}\left(\frac{V}{R_0 + R_c}\right)^2 \tag{4}$$

The current through the nanowire (plus its junctions) is given by

$$i = \frac{V}{R_0 + R_c} \tag{4'}$$

We define R_{cM} as the resistance of the nanowire when it is in the metallic state, i.e., when the temperature of the nanowire is above the Mott transition temperature T_M, and R_{cD} as the nanowire resistance when the temperature of the nanowire is below T_M. Rearranging eq 4, the two values of the voltage at which the nanowire's temperature is T_M, $V_M^{\uparrow}$ and $V_M^{\downarrow}$, are given by

$$V_M^{\uparrow} = \left[\frac{k(T_M - T_0)(R_0 + R_{cD})^2}{R_{cD}}\right]^{1/2} \tag{5}$$

$$V_M^{\downarrow} = \left[\frac{k(T_M - T_0)(R_0 + R_{cM})^2}{R_{cM}}\right]^{1/2} \tag{5'}$$

where, in eqs 5 and 5′, the up and down values of V_M relate respectively to the two values of R_c. Two limits can be defined. The pertinent one is the case where the contact resistance is low compared with the nanowire resistance both in its insulator and metallic states. In that case

$$V_M^{\uparrow} = [k(T_M - T_0)R_{cD}]^{1/2} \tag{6}$$

$$V_M^{\downarrow} = [k(T_M - T_0)R_{cM}]^{1/2} \tag{6'}$$

Since $R_{cM} \ll R_{cD}$, $V_M^{\uparrow} > V_M^{\downarrow}$, as observed (Figure 3a). The other limit to be considered is one in which the contact resistance is very large compared to the nanowire's resistance both in its insulator and metallic state; then according to eq 4′ the current is more or less independent of the Mott transition. (More complicated cases arise when the contact resistance is larger than the nanowire's resistance when the nanowire is in its metallic state but small compared to its resistance in its insulator state. The dependence of the current on voltage in those cases can be determined by using eqs 5 and 5′. Equations 5, 5′, 6, and 6′ also show how the transition voltages would depend on raising or lowering the ambient temperature T_0. Increasing the ambient temperature would decrease V_M because the ambient temperature affects the nanowire's carrier density both below and above the Mott transition leading to interesting and useful thermo-electrical phenomena.

Using eq. 6 and 6′, the difference in the square of the voltages at which the Mott transition occurs in the upward and downward directions is proportional to the difference between the Mott transition temperature and the ambient temperature.

$$V_M^{\uparrow 2} - V_M^{\downarrow 2} \propto (T_M - T_0) \tag{7}$$

That is, a plot of ΔV_M^2 vs T_0 should give a straight line with negative slope and an intercept T_M. This is, in fact, observed. An example is shown in Figure 3a for one of the nanowires studied, for which the Mott transition temperature was found to be 67.5 (±0.9) °C.

The values of T_M determined in the above manner for 14 individual nanowires are shown in Figure 3. The set of values linearly correlate (correlation coefficient = $R^2 = 0.42$) with the lateral dimension of the nanowires (Figure 4) as measured at the nanowire-substrate interface. In contrast to this, the correlations between T_M and the length ($R^2 = 0.08$) and height ($R^2 = 0.07$) of the nanowires are very poor. For all of the nanowires, the measured heights, i.e., the dimension measured normal to the substrate, were always smaller than their widths and also less broadly distributed. (Of course, there is no basis in physics

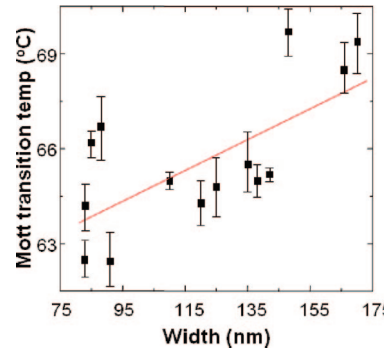

Figure 4. The Mott transition temperatures, determined as illustrated in Figure 3b as a function of the lateral dimension (width) of several VO_2 nanowires ranging in value from 80 to 170 nm. The Mott transition temperature trends downward with decreasing nanowire width. However, the scatter in T_M values exceeds the experimental error, implying that, while T_M seems to correlate with the lateral dimension of the nanowire (at least for nanowires in contact with SiO_2), other nanowire parameters also affect the value of T_M. The vertical bars denote the calculated experimental error determined from the fit to eq 5.

for a linear dependence of T_M on the nanowire width. The significant scatter in the data makes a fit to an actual model inappropriate, and only a consideration of the trend as indicated by a linear correlation is justified.)

The measured values of T_M ranged from ~62 to 70 °C. A linear fit of T_M vs the reciprocal of the lateral dimension yielded an intercept value of $T_M = 70.7$ °C which, on the basis of such a plot, corresponds to the Mott transition value at infinite width. This value is a little larger than most reported values of the Mott transition temperatures for macroscopic samples of VO_2 but not excessively so.[1,2] The results also show that T_M tends to decrease with the decreasing width of the quasi-one-dimensional VO_2 nanowire.

The observed correlation of T_M with the lateral dimension but not with nanowire height probably suggests that the observed size effect on the value of T_M is due to the interaction between the nanowire and the substrate. A substrate effect of this sort wherein the strain arising from VO_2−substrate interactions result in alternating domains of metal and insulator regions of the VO_2 along the length of the nanowire was previously described.[16] However, the rather complex current vs temperature behavior reported in that study, which showed multiple transitions explained as strain induced periodic metal−insulator domain formation, was not observed in our study. We speculate that the much reduced growth temperature (650 vs 1100 °C) in comparison to ref 15 account for the absence of strain induced domains. It is also clear that for the nanowires investigated in the present study T_M depends on other parameters besides the interaction between the nanowire and its substrate since the scatter in the values of T_M shown in Figure 4 exceeds the experimental error inherent in the determination of T_M.

The VO_2 nanowires are produced at high temperatures, when they are in the metallic (tetragonal) phase. As the system cools below the Mott transition temperature, two strain inducing processes ensue. Assuming that the interaction between the nanowire and the silica substrate is significant, strain is induced at that interface due to the differing thermal expansion characteristics between VO_2 and silica.[3,17] Second, as the system's temperature falls below the Mott transition temperature the VO_2 changes phase to monoclinic further modifying the substrate-induced stress on the nanowire. This is likely the reason why the nanowire shows sharp corners at the silica-VO_2 interface but rounded corners at the nanowire-air interface: the strong interaction between the silica and the VO_2 prevents the restructuring to occur fully at that interface, while at the opposite interface, the VO_2−air interface, the crystal habit of the monoclinic phase is more fully accommodated.

According to the above view, strain would be relieved in the nanowire/substrate system when the nanowire undergoes the Mott transition into its metallic phase. This would translate into a width-dependent value of T_M, according to the interplay between stresses at the interface and stresses in the bulk that extend from the interface into the volume of the nanowire. If the strain at the nanowire-substrate interface extends more deeply into the bulk for the narrower nanowires than for the broader nanowires, a not unreasonable possibility, then the magnitude of the free energy change accompanying the phase transition would be greater for the narrower nanowires than for the broader ones, encouraging the system to undergo the transition at a lower temperature.

Conclusions

In summary, single-crystal VO_2 nanowires were synthesized using atmospheric-pressure, physical vapor deposition. Current−voltage measurements were carried out on individual nanowires outfitted with metal electrodes fashioned by optical lithography and metal vapor deposition. The Mott insulator-to-metal transition temperatures of several nanowires with varying lateral dimensions were determined by measuring the voltage values at which sharp a current step, signaling that the occurrence of the insulator-to-metal or the reverse transition, had taken place. At those voltage values, the temperature of the nanowire corresponded to the Mott transition temperature. The observed Mott transition temperatures showed an overall downward trend with decreasing nanowire width. We ascribe this to strong interactions between the nanowire and the underlying silica substrate. However, the Mott-temperature versus nanowire width correlation was poor, indicating that other parameters, likely the nanowire's metal/oxygen stoichiometry and defect structure, also contribute to value of the Mott transition temperature of nanostructured VO_2.

Acknowledgment. This work was supported by the Institute for Collaborative Biotechnologies through Grant DAAD19-03-D- 0004 from the U.S. Army Research Office and made extensive use of the MRL Central Facilities at UCSB supported by the National Science Foundation under Award Nos. DMR-0080034 and DMR-0216466 for the HRTEM/STEM microscopy. We gratefully acknowledge the financial support from the Partnership for International Research and Education, for Electronic Chemistry and Catalysis at Interfaces, NSF Grants No. OISE-0530268.

References and Notes

(1) Eyert, V. *Ann. Phys. (Berlin, Ger.)* **2002**, *11*, 650–704.
(2) Biermann, S.; Poteryaev, A.; Lichtenstein, A. I.; Georges, A. *Phys. Rev. Lett.* **2005**, *94*, 026404.
(3) Rakotoniaina, J. C.; Mokranitamellin, R.; Gavarri, J. R.; Vacquier, G.; Casalot, A.; Calvarin, G. *J. Solid State Chem.* **1993**, *103*, 81–94.
(4) Greenberg, C. B. *Thin Solid Films* **1994**, *251*, 81–83.
(5) Chudnovskiy, F.; Luryi, S.; Spivak, B. In *Future Trends in Microelectronics: The Nano Millenium*; Luryi, S., Xu, J. M., Zaslavsky, A., Eds.; Wiley-Interscience: Hoboken, NJ, 2002; pp 148−155.
(6) Kim, H. T.; Chae, B. G.; Youn, D. H.; Maeng, S. L.; Kim, G.; Kang, K. Y.; Lim, Y. S *New J. Phys* **2004**, *6*, 51–59.
(7) Pouget, J. P.; Launois, H.; D'Haenens, J. P.; Merenda, P.; Rice, T. M. *Phys. Rev. Lett.* **1975**, *35*, 873–875.
(8) Lopez, R.; Feldman, L. C.; Haglund, R. F. *Phys. Rev. Lett.* **2004**, *93*, 177403.
(9) Boriskov, P. P.; Velichko, A. A; Stefanovich, G.B. *Phys. Solid State* **2004**, *46*, 922–926.
(10) Kim, H.-T.; Chae, B.-G.; Youn, D.-H.; Kim, G.; Lee, S.-J.; Kim, K.; Lim, Y.-S.; Kang, K.-Y. *Appl. Phys. Lett.* **2005**, *86*, 242101.
(11) Baik, J. M.; Lee, J. L. *Adv. Mater.* **2005**, *17*, 2745–2748.
(12) Manning, T. D.; Parkin, I. P.; Clark, R. J. H.; Sheel, D.; Pemble, M. E.; Vernadou, D. *J. Mater. Chem.* **2002**, *12*, 2936–2939.
(13) Schilbe, P. *Physica B* **2002**, *316* (317), 600–602.
(14) Khakhaev, I. A.; Ghudnovskii, F. A.; Shadrin, E. B. *Phys. Solid State* **1994**, *36*, 898.
(15) Guiton, B. S.; Gu, Q.; Prieto, A. L.; Gudiksen, M. S.; Park, H. *J. Am. Chem. Soc.* **2005**, *127*, 498–499.
(16) Wu, J.; Gu, Q; Guiton, B. S.; de Leon, N. P.; Ouyang, L.; Park, H. *Nano Lett* **2006**, *6*, 2313–2317.
(17) Lopez, R.; Boatner, L. A.; Haynes, T. E.; Haglund, R. F.; Feldman, L. C. *Appl. Phys. Lett.* **2001**, *79*, 3161–3163.

JP805537R